Formation of a Three-Dimensional Network of V Trimers in $A_2V_{13}O_{22}$ (A = Ba, Sr)

J. Miyazaki,[1] K. Matsudaira,[2] Y. Shimizu,[2,3] M. Itoh,[2] Y. Nagamine,[4] S. Mori,[4] J. E. Kim,[5] K. Kato,[5,6] M. Takata,[5,6] and T. Katsufuji[1,7,8,*]

[1]*Department of Physics, Waseda University, Tokyo 169-8555, Japan*
[2]*Department of Physics, Nagoya University, Nagoya 464-8601, Japan*
[3]*Institute for Advanced Research, Nagoya University, Nagoya 464-8601, Japan*
[4]*Department of Materials Science, Osaka Prefecture University, Sakai 599-8531, Japan*
[5]*Japan Synchrotron Radiation Research Institute, Hyogo 679-5198, Japan*
[6]*RIKEN SPring-8 Center, Hyogo 679-5148, Japan*
[7]*Kagami Memorial Laboratory for Material Science and Technology, Waseda University, Tokyo 169-0051, Japan*
[8]*PRESTO, Japan Science and Technology Corporation, Saitama 332-0012, Japan*

(Received 3 February 2010; published 18 May 2010)

We found that in $A_2V_{13}O_{22}$ (A = Ba, Sr), which contains a trilayer slab of VO in the sodium-chloride structure with periodically missing ions, the trimerization of V ions occurs at 290 K (A = Ba) and 380 K (A = Sr). V trimers form a three-dimensional network, but some V ions remain untrimerized in these compounds. The suppression of magnetic susceptibility with trimerization and the existence of a Curie tail at low temperatures, together with the result of NMR measurement, indicate that the V trimers are spin singlet, whereas the untrimerized V ions have a magnetic moment; i.e., there is a spontaneous separation between nonmagnetic and magnetic ions in the crystal.

DOI: 10.1103/PhysRevLett.104.207201 PACS numbers: 75.25.Dk, 61.50.Ks, 71.30.+h, 76.60.Cq

The spontaneous formation of high-order structures in a crystal is a characteristic behavior in transition-metal oxides. A well-known example of high-order structures is a stripe phase with charge ordering observed in cuprates [1], manganites [2], and nickelates [3]. In this stripe phase, carriers (electrons or holes) are condensated into periodically aligned stripes below the transition temperature. The transition into a stripe phase often induces an increase in electrical resistivity and a suppression of magnetic susceptibility as macroscopic properties. Another example of high-order structures is a cluster of transition-metal ions. A simple example of such a cluster is a dimer associated with, for example, a spin- Peierls transition [4]. In this case, two electrons originating from two transition-metal ions form a spin-singlet state in a dimer, and this dimer becomes a building block of a high-order structure in a spin-singlet ground state.

Building blocks composed of more than three ions are also known, for example, trimers in $LiVO_2$ [5] and $LiVS_2$ [6], tetramers in $MgTi_2O_4$ [7,8], heptamers in AlV_2O_4 [9], and octamers in $CuIr_2S_4$ [10], but they are fairly rare, and in most cases, the alignment of the building block in the crystal is simple, a linear or planar alignment. In this Letter, we report a new type of high-order structures, which is a three-dimensional network of trimers in a modified fcc lattice of V ions in $A_2V_{13}O_{22}$ (A = Ba, Sr). The crystal structure of these compounds is based on the sodium-chloride structure of V and O, i.e., the face-centered-cubic (fcc) structure of the V ions surrounded by edge-sharing oxygen octahedra. In such a crystal structure, there is a direct overlap of the t_{2g} orbital between the nearest-neighbor transition metals, as shown in Fig. 1(c). The formation of the spin-singlet V trimers in the present compounds can be attributed to the orbital ordering of the t_{2g} states, i.e., the bond formation of the t_{2g} orbitals at each side of the triangle.

Polycrystalline samples of $A_2V_{13}O_{22}$ were synthesized by solid-state reaction. Appropriate amounts of $Ba_2V_2O_7$ ($Sr_2V_2O_7$), V_2O_3, and V were mixed, pressed into pellets and sintered in a sealed quartz tube at 1200 °C for 24 h. Electrical resistivity was measured by a four-probe technique. Magnetic susceptibility was measured by a SQUID magnetometer. An electron diffraction experiment was carried out in the temperature window between 298 and 100 K in a JEM-2010 transmission electron microscope operating at 200 kV. Synchrotron x-ray powder diffraction measurement was performed with an incident wavelength of 0.7776 Å at SPring-8 BL02B2 [11]. The Rietveld analysis of the diffraction data was conducted with Rietan-2000 [12]. ^{51}V NMR spectra were obtained by the Fourier transformation of spin-echo signals.

The present compound, $A_2V_{13}O_{22}$, has not been synthesized so far, though $Ba_2Ti_{13}O_{22}$ with the same crystal structure is a known compound [13]. We have determined the crystal structure of $A_2V_{13}O_{22}$ by the Rietveld analysis of the synchrotron x-ray powder diffraction [14]. Here, we focus on the arrangement of the V ions in the crystal structure of $A_2V_{13}O_{22}$. It is orthorhombic (space group is $Cmce$) at room temperature and can be regarded as a trilayer structure. In the first layer ($z = 2/6$), the V ions form a lattice where V "boats," each of which is composed of five V ions, are connected to each other along the ab plane, as shown in Fig. 1(a). This V lattice can be regarded as the V triangular lattice from which V triangles [shown

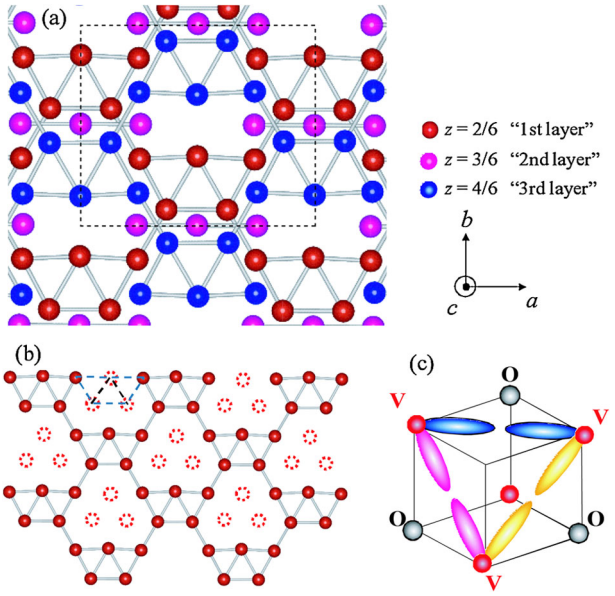

FIG. 1 (color online). (a) Arrangement of V ions (spheres) in $A_2V_{13}O_{22}$ on $z = 2/6$, $3/6$, and $4/6$ layers. The dashed line indicates the unit cell. (b) Arrangement of V ions on $z = 2/6$ layer. Dashed circles indicate the V triangles missing from the triangular lattice. Dashed lines indicate the position of the V boat on the $z = 1/6$ layer. (c) xy, yz, or zx orbitals extending along each side of the V triangle. The figures of the crystal structure were drawn by VESTA K. Momma and F. Izumi, J. Appl. Crystallogr. **41**, 653 (2008).

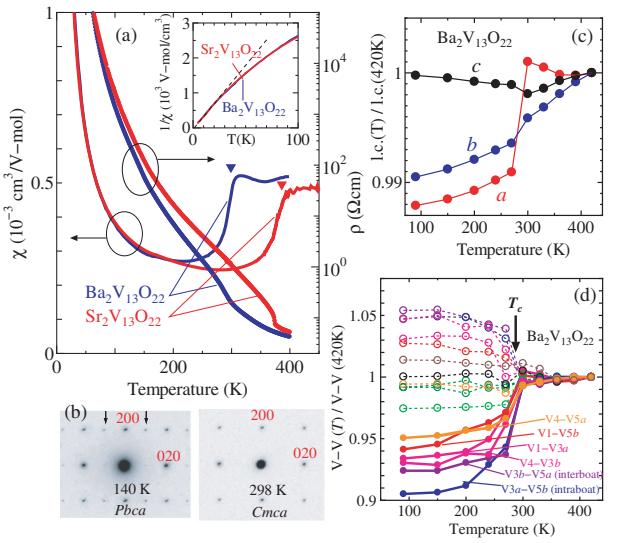

FIG. 2 (color online). (a) Temperature dependence of resistivity (right axis) and magnetic susceptibility measured at 0.1 T (left axis) for $Ba_2V_{13}O_{22}$ and $Sr_2V_{13}O_{22}$. The inset shows the inverse magnetic susceptibility. The dashed line in the inset indicates the Curie-Weiss behavior expected when an $S = 1/2$ spin exists on the V2 site. (b) [001] zone-axis electron diffraction patterns of $Ba_2V_{13}O_{22}$ above and below $T_c = 290$ K. Arrows indicate the reflection forbidden in the high-temperature phase. (c) Temperature dependence of lattice constants in $Ba_2V_{13}O_{22}$. (d) Temperature dependence of bond length of all nearest-neighbor V-V sites. The obtained data are normalized to the values at 420 K. Solid lines and solid circles refer to the six V-V bonds that exhibit large contractions with the phase transition.

by the dotted circles in Fig. 1(b)] are periodically missing. The third layer ($z = 4/6$) is the same as the first layer, except for the opposite direction of the boats. In the second layer ($z = 3/6$), V "bars," each of which is composed of three V ions in the straight and sits between the two boats on the first and third layers, are periodically aligned. This second layer can also be regarded as the V triangular lattice from which V ions are periodically missing. The stacking of these three layers as the triangular lattices is the same as the stacking of the triangular lattice in the fcc lattice along the diagonal direction, i.e., ABC-type stacking. Between $z = 2/6$ and $z = 1/6$, i.e., between one trilayer ($z = 2/6$, $3/6$, $4/6$) and the next trilayer ($z = -1/6$, 0, $1/6$), the position of the boat is shifted by $x = 1/2$, as shown in Fig. 1(b) by dashed lines, and thus, there is only a small intertrilayer interaction. Therefore, this compound can be regarded as consisting of the trilayer slab of VO in the sodium-chloride structure (V on the fcc lattice), from which V and O ions are periodically missing. The average valence of V is $3\frac{1}{13}$ in $A_2V_{13}O_{22}$, and thus, nominally 12 out of 13 V ions are 3+ ($3d^2$), and the remaining one is 4+ ($3d^1$), and there are 25 electrons in 13 V.

Figure 2(a) shows the temperature (T) dependence of resistivity [$\rho(T)$, right axis] and magnetic susceptibility [$\chi(T)$, left axis] for $Ba_2V_{13}O_{22}$ and $Sr_2V_{13}O_{22}$. There are anomalies in $\rho(T)$ at 290 K for $Ba_2V_{13}O_{22}$ and at 380 K for $Sr_2V_{13}O_{22}$, and $\rho(T)$ diverges at low temperatures. It was found that the $\rho(T)$ for $T < 100$ K almost follows an activation-type T dependence, $\rho = \rho_0 \exp(\Delta/k_BT)$, with $\Delta \sim 0.05$ eV both for $Ba_2V_{13}O_{22}$ and $Sr_2V_{13}O_{22}$, indicating insulating states at low T in these compounds. The $\chi(T)$ of $A_2V_{13}O_{22}$ is almost T independent at high T, but it exhibits a large reduction at the temperature where $\rho(T)$ exhibits the anomaly. At low temperatures ($T < 200$ K), the $\chi(T)$ of $A_2V_{13}O_{22}$ increases and obeys a Curie-Weiss law below ~50 K, as shown in the inset. These results indicate that there are phase transitions in $A_2V_{13}O_{22}$ (A = Ba, Sr), and their low T phases are insulating states with substantially suppressed magnetic moments.

To understand the phase transition in $A_2V_{13}O_{22}$, the change in crystal structure at the phase transition was studied by synchrotron x-ray powder diffraction and electron diffraction measurements. A sudden shift of the synchrotron x-ray diffraction peaks was observed at $T_c = 290$ K for $Ba_2V_{13}O_{22}$ and at 380 K for $Sr_2V_{13}O_{22}$. In addition, new peaks, which are forbidden in the space group $Cmce$, appear below T_c. A more comprehensive study to determine the space group below T_c was performed by electron diffraction measurement, a part of which is shown in Fig. 2(b), and it was concluded that the space group changes from $Cmce$ to $Pbca$ with the phase transition [14]. This change in space group is the same as that observed in $BaV_{10}O_{15}$ [15], which takes a

bilayer structure composed of only the first and third layers (without the second layer) of $A_2V_{13}O_{22}$.

The T dependence of the lattice constants in $Ba_2V_{13}O_{22}$ [normalized to the values at 420 K, $a = 11.495(1)$ Å, $b = 9.8892(1)$ Å, $c = 13.9344(2)$ Å] obtained from the analysis of the x-ray diffraction is shown in Fig. 2(c), where the a and b lattice constants decrease, and the c lattice constant increases at 290 K. It should be noted that there is also an anomalous T dependence above $T_c = 290$ K; the a axis increases with decreasing T below 350 K. Although the origin of such T dependence is unknown, this seems to correspond to the small but distinct T dependence of $\chi(T)$ in the same compound in the same T range (300–400 K) shown in Fig. 2(a).

In Fig. 2(d), the lengths of all the inequivalent nearest-neighbor V-V bonds of $Ba_2V_{13}O_{22}$ are plotted. Among these bonds, six bonds exhibit large contractions (by 4–9%) with the structural phase transition, as indicated by solid lines and circles. We plot the absolute values of the bond length above and below T_c in Figs. 3(a) and 3(b), in which those short six bonds are highlighted. As can be seen, the 6 V-V bonds form trimers in the V lattice. Here, there are two types of V trimers: one is either within the first or third layer of the trilayers with the normal vector parallel to the c axis, and the other straddles either in the first and second layers or in the third and second layers. As illustrated in the box, the latter (straddling two layers) is also in the shape of a nearly regular triangle. It should be noted that the center of the three V ions in the second layer (V2) does not belong to any trimers. Therefore, 13 V ions are separated into four V trimers in a three-dimensional network and one untrimerized V ion in the low-T phase of $A_2V_{13}O_{22}$.

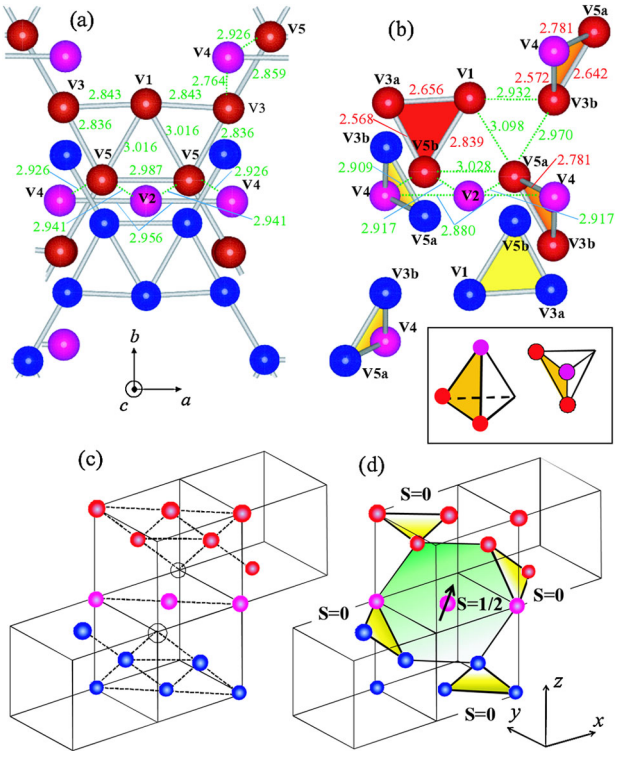

FIG. 3 (color online). (a), (b) Arrangement of V ions and V-V bond lengths in Å for $Ba_2V_{13}O_{22}$. (a) at 420 K $> T_c$ and (b) at 90 K $< T_c$. The typical error of the bond length is ± 0.008 Å. Filled triangles in (b) correspond to V trimers. (c), (d) Illustration of V ions in $A_2V_{13}O_{22}$ on fcc lattice (c) above and (d) below T_c.

One can look at the arrangement of the V ions in $A_2V_{13}O_{22}$ and the V trimerization on the fcc lattice in Figs. 3(c) and 3(d). In the high-T phase [Fig. 3(c)], V boats are on the (111) plane, and a V bar exists in between. In the low-T phase [Fig. 3(d)], four trimers, each of which is composed of one V ion at the corner and two V ions at the face center of the fcc lattice, surrounds the untrimerized V ion in a hexagonal shape.

This V trimerization is caused by the bond formation of the t_{2g} orbitals, as proposed for the trimerization in $LiVO_2$ [5]. Between the nearest-neighbor V ions on the fcc lattice, either xy, yz, or zx orbitals from the two V ions have an overlap [Fig. 1(c)]. Thus, at each side of the trimers in $A_2V_{13}O_{22}$, there is a bonding state, which can accommodate two d electrons in a spin-singlet state. Accordingly, 24 d electrons can be accommodated in four trimers in a spin-singlet state, and there remains one (=25–24, where 25 is the number of d electrons in 13 V) d electron in the untrimerized V ion. This spin-singlet formation of the V d electrons associated with the trimerization leads to the reduction in magnetic susceptibility at T_c. On the other hand, the untrimerized V ion with one d electron should have a spin with $S = 1/2$. The Curie constants estimated from the behavior of $1/\chi(T)$ below 25 K shown in the inset of Fig. 2(a), namely, 2.9×10^{-2} and 2.7×10^{-2} cm^3 K/V mol for A = Ba and Sr, respectively, are consistent with the value obtained when there is a $S = 1/2$ spin at one out of 13 V ions (2.88×10^{-2} cm^3 K/V mol). This result strongly supports our model, indicating that the V trimers are spin singlet, but the untrimerized V ions have magnetic moments.

Figure 4(a) shows the ^{51}V-NMR spectra at 9.4026 T at various temperatures. The anisotropic line shape above $T_c = 290$ K is explained by a powder pattern with an anisotropic Knight shift and a negligibly small nuclear quadrupole interaction. The peak suddenly shifts to higher frequencies at T_c and then exhibits a continuous shift in the same direction and a broadening with decreasing T. Figure 4(b) shows the T dependence of the ^{51}V Knight shift (K) obtained from the peak of the NMR spectrum. K is given by the sum of the T-independent orbital (Van Vleck) term and the spin term. Since the hyperfine coupling constant from the on-site electrons is *negative*, a sudden decrease in $-K$ at $T_c = 290$ K corresponds to a decrease in local spin susceptibility, which is consistent with $\chi(T)$ shown in Fig. 2(a). It should be noted that the NMR signal below T_c originates only from the V sites in the spin-singlet state whereas the signal from the magnetic sites with a high relaxation rate would be wiped out from

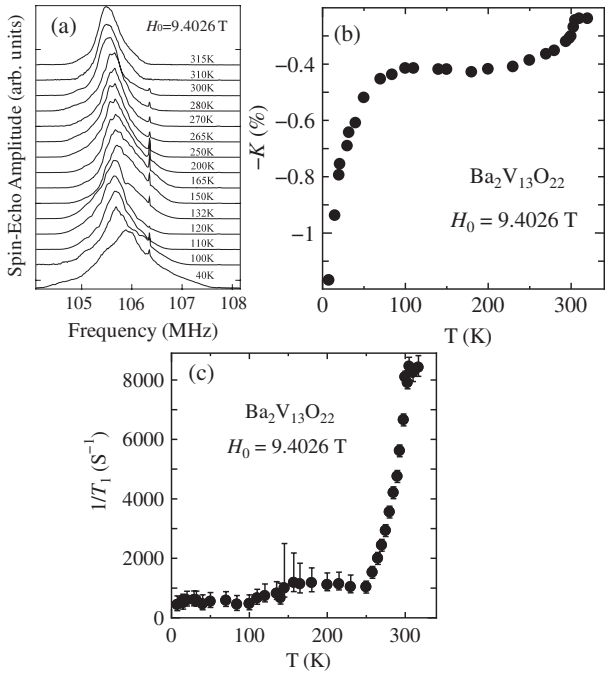

FIG. 4. (a) ^{51}V-NMR spectra at 9.4026 T at various temperatures. (b) Temperature dependence of Knight shift $-K$. (c) Temperature dependence of nuclear spin-lattice relaxation rate $1/T_1$.

the spectrum. On the other hand, a further decrease in $-K$ (i.e., an increase in K) at low temperatures (<100 K) and the broadening of the spectra should be ascribed to the *positive* transferred hyperfine fields from the neighboring paramagnetic spins. Namely, although the signal from the magnetic sites itself cannot be observed, the spins on those sites, whose susceptibility is enhanced in a Curie-Weiss manner at low T, affect the signal from the neighboring nonmagnetic sites through positive transferred hyperfine fields. The different behaviors of $-K(T)$, which decreases at $T_c = 290$ K and further decreases below 100 K, and $\chi(T)$, which decreases at $T_c = 290$ K but increases below 100 K, are caused by the different signs of the hyperfine coupling constants from the on-site electrons and from the electrons on the neighboring sites. Therefore, the present NMR result gives microscopic evidence for the coexistence of spin-singlet and magnetic V ions.

The T dependence of nuclear spin-lattice relaxation rate $1/T_1$ is shown in Fig. 4(c). A large decrease in $1/T_1$ below T_c is observed, which is consistent with the spin-gap formation. The critical slowing down in T_1, i.e., the increase in $1/T_1$, which is indicative of the long-range magnetic order, was not observed down to 7.5 K, indicating that the spins on the magnetic V ions do not order down to low temperatures.

One characteristic of the ground state of $A_2V_{13}O_{22}$ is that V ions are spontaneously separated into nonmagnetic ions (trimers) and magnetic ions. Such a spontaneous separation of the nonmagnetic and magnetic ions is observed in AlV_2O_4 with a spinel structure [9,16], in which eight V ions are separated into nonmagnetic heptamers (seven V ions) and one magnetic V ion, and in $SrV_xGa_{12-x}O_{19}$ with a magnetoplumbite structure [17], in which the V ions on the kagome lattice form nonmagnetic (spin-singlet) trimers, whereas those on the triangular lattice between two kagome layers remain magnetic. In $BaV_{10}O_{15}$, which can be regarded as a bilayer version of $Ba_2V_{13}O_{22}$, a separation of spin-singlet V trimers and magnetic V ions, which antiferromagnetically order at low temperatures, has been proposed [18]. These results indicate the stability of spin-singlet trimers for the V^{3+} ($3d^2$) ions on the triangle-based lattice.

In summary, we synthesized and studied the transport, magnetic, and structural properties of $A_2V_{13}O_{22}$ (A = Ba, Sr). We found that there is a phase transition at 290 K (Ba) and 380 K (Sr), which is dominated by the formation of V trimers in a three-dimensional network. These V trimers are in a spin-singlet state caused by the orbital ordering of t_{2g} states, whereas the untrimerized V ions have a magnetic moment.

We thank T. Oguchi for fruitful discussion. This work was partly supported by Grants-in-Aid for Scientific Research on Priority Areas (20046014) and "Academic Frontier" Project from MEXT and Scientific Research B (21340105) from JSPS of Japan. The synchrotron radiation experiments were performed at BL02B2 in SPring-8 with the approval of the Japan Synchrotron Radiation Research Institute (JASRI) (Proposal No. 2009B1068).

*To whom correspondence should be addressed.

[1] J. M. Tranquada *et al.*, Nature (London) **375**, 561 (1995).
[2] S. Mori, C. H. Chen, and S.-W. Cheong, Nature (London) **392**, 473 (1998).
[3] C. H. Chen, S.-W. Cheong, and A. S. Cooper, Phys. Rev. Lett. **71**, 2461 (1993).
[4] M. Hase, I. Terasaki, and K. Uchinokura, Phys. Rev. Lett. **70**, 3651 (1993).
[5] H. F. Pen *et al.*, Phys. Rev. Lett. **78**, 1323 (1997).
[6] N. Katayama *et al.*, Phys. Rev. Lett. **103**, 146405 (2009).
[7] M. Schmidt *et al.*, Phys. Rev. Lett. **92**, 056402 (2004).
[8] D. I. Khomskii and T. Mizokawa, Phys. Rev. Lett. **94**, 156402 (2005).
[9] Y. Horibe *et al.*, Phys. Rev. Lett. **96**, 086406 (2006).
[10] P. G. Radaelli *et al.*, Nature (London) **416**, 155 (2002).
[11] E. Nishibori *et al.*, Nucl. Instrum. Methods Phys. Res., Sect. A **467–468**, 1045 (2001).
[12] F. Izumi and T. Ikeda, Mater. Sci. Forum **321–324**, 198 (2000).
[13] J. Akimoto *et al.*, J. Solid State Chem. **113**, 384 (1994).
[14] See supplementary material at http://link.aps.org/supplemental/10.1103/PhysRevLett.104.207201 for the details in the study of the crystal structure.
[15] C. A. Bridges and J. E. Greedan, J. Solid State Chem. **177**, 1098 (2004).
[16] Y. Shimizu *et al.*, Phys. Rev. B **78**, 144423 (2008).
[17] J. Miyazaki *et al.*, Phys. Rev. B **79**, 180410(R) (2009).
[18] T. Kajita *et al.*, Phys. Rev. B **81**, 060405(R) (2010).